Complex geophysical wake flows

Rui Miguel A. Caldeira & Pablo Sangrà

Ocean Dynamics
Theoretical, Computational and
Observational Oceanography

ISSN 1616-7341
Volume 62
Number 5

Ocean Dynamics (2012) 62:683-700
DOI 10.1007/s10236-012-0528-6

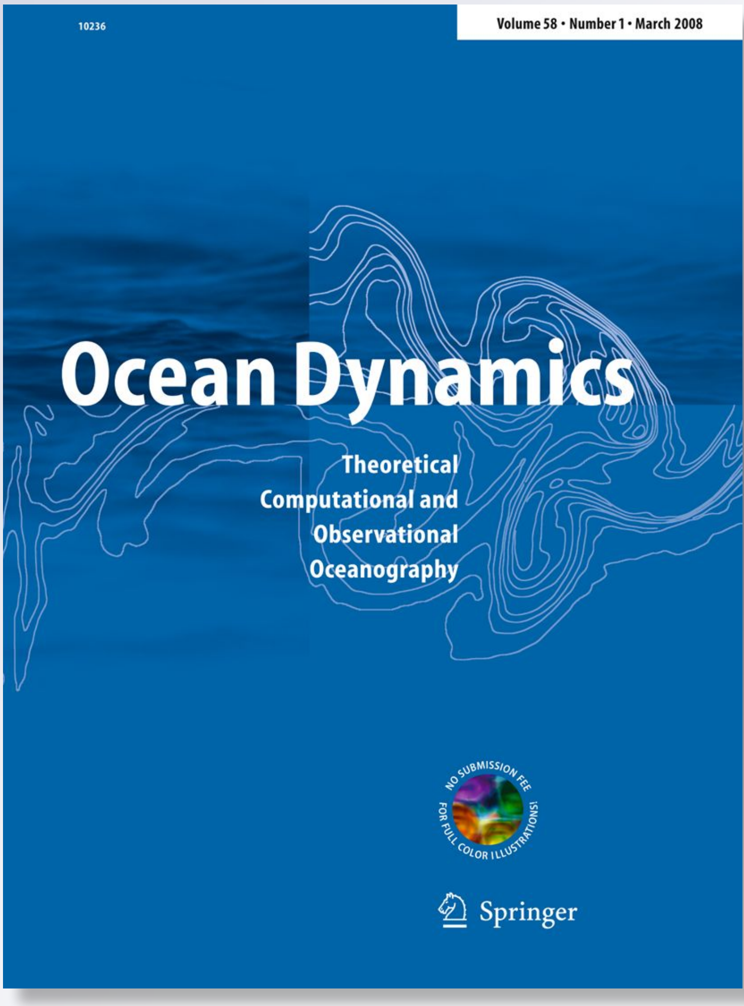

Springer

Ocean Dynamics (2012) 62:683–700
DOI 10.1007/s10236-012-0528-6

Complex geophysical wake flows

Madeira Archipelago case study

Rui Miguel A. Caldeira · Pablo Sangrà

Received: 24 June 2011 / Accepted: 3 February 2012 / Published online: 11 March 2012

Abstract Idealized studies of island wakes often use a cylinder-like island to generate the wake, whereas most realistic studies use a close representation of the oceanic bathymetry immersed in a complex representation of the "ambient" geophysical flows. Here, a system of multiple islands was placed into numerical and experimental channels, in order to focus on the complexity of the archipelago wake, including (a) the influence of small neighboring islands and (b) the role of the island-shelf. The numerical geostrophic and stratified channel was built using a three-dimensional primitive equation model, considering a realistic representation of the Madeira archipelago bathymetry, with prescribed initial and boundary conditions. Results from the simulations show that the neighboring islands alter the near-field wake. Small eddies generated by the neighboring islands lead to destabilization of the shear layers of the larger island. Laboratory experiments carried out in the Coriolis rotating tank corroborated this near-field disruptive mechanism. The neighboring island perturbation effect was present whatever the direction of the incoming flow, but under different regimes. North–south wakes produced geostrophic eddies ($\geq R_{\mathrm{d}}$), whereas west–east wakes produced (exclusively) ageostrophic submesoscale eddies ($<<R_{\mathrm{d}}$) which traveled offshore with wave-like motion. The archipelago shelf contributed to the asymmetric vertical migration of oceanic vorticity. Cyclonic vorticity dominated the surface dynamics, whereas anticyclonic circulation prevailed at the bottom part of the linearly stratified upper layer. This study identifies several likely wake scenarios induced by the Madeira archipelago, and may serve as guide for future multiscale numerical studies and in situ campaigns.

Keywords Island wake · Submesoscale eddies · Boundary layer disruption · Hydrodynamic drafting · Topographic trapped waves · Vertical shear · Subinertial instabilities

Responsible Editor: Emil Vassilev Stanev

Electronic supplementary material The online version of this article (doi:10.1007/s10236-012-0528-6) contains supplementary material, which is available to authorized users.

R. M. A. Caldeira (✉)
CIIMAR—Interdisciplinary Centre of Marine and Environmental Research, Rua dos Bragas, 289, 4050-123 Porto, Portugal
e-mail: rcaldeira@ciimar.up.pt

R. M. A. Caldeira
CCM—Center for Mathematical Sciences, Universidade da Madeira, Campus Universitário da Penteada, 9000-390 Funchal, Madeira, Portugal
URL: http://wakes.uma.pt

P. Sangrà
Departamento de Fisica, Edificio de Ciencias Basicas, Universidad de Las Palmas de Gran Canaria, Campus Universitario de Tafira, 35002, Las Palmas, Gran Canaria, Spain

1 Introduction

Several classical studies have discussed on the deep-ocean island wake problem (e.g., Tomczak 1988; Heywood et al. 1996; Dietrich et al. 1996). For the deep-sea island case, most of the frictional forces inducing wake formation originate from the (near-field) island coastal boundary, whereas for a shallow water wake, the surface and bottom boundary Ekman layers are equally important (e.g., Tomczak 1988). For a deep-ocean island, frictional effects induced by the surface and bottom boundary layers are often neglected, specially considering the Ekman layer depth << than the surrounding total depth (H). In the coastal ocean, however, the Ekman layer and water depth are comparable in size and therefore must be considered (e.g., Tomczak 1988).

Shallow water wakes have been well described, with studies of islands located on continental shelves such as the small islands of the Great Barrier Reef, Australia (e.g., Wolanski et al. 1984, 1996; Furukawa and Wolanski 1998; White and Wolanski 2008). The deep-ocean island wake problem has also received much attention; at the Canary Archipelago (e.g., Aristegui et al. 1994; Barton et al. 2000; Sangra et al. 2007), at the islands of the Southern California Bight (e.g., Caldeira et al. 2005; Dong et al. 2007) as well as elsewhere (Coutis and Middleton 2002). In all cases, notions underlying the physics of wake flow instabilities inherit concepts developed from laboratory and idealized numerical experiments (e.g., Boyer and Davies 2000; Perret et al. 2006; Teinturier et al. 2010).

Idealized studies of island wakes often use a cylinder-like island to generate the wake (e.g., Dong et al. 2007), whereas most "realistic" studies use a close representation of the oceanic bathymetry (e.g., Dong and McWilliams 2007; Calil et al. 2008). Here, we attempt to construct a (semi)realistic wake built in a "block-by-block" fashion, that is, first considering the (asymmetric) Madeira Island and secondly including a representative bathymetry of the whole archipelago, i.e., Madeira, Desertas, and Porto Santo. Preliminary studies suggested that the Selvage Islands were sufficiently far from Madeira to generate independent wakes. Since the oceanographic setting of the Madeira Archipelago region is not well documented (see Section 2), there was an added concern to consider several probable oceanic scenarios, taking into account the different directions and intensities of the incoming flow. Nevertheless, the discussion herein is focused on fully developed wake cases, i.e., Von Karman vortex streets.

Apart from the discussions in the oceanographic scientific literature, there is a large body of work including experimental and/or numerical discussions on wakes forming behind bluff bodies in non-stratified fluids. The suppression of vortex shedding due to the presence of a control cylinder is a topic not commonly discussed in the oceanographic literature, but which continues to generate comprehensive debate in the fluid mechanics community (e.g., Strykowski and Sreenivasan 1990; Sakamoto et al. 1991; Dalton et al. 2001; Kuo et al. 2007; Parezanovića and Cadot 2009).

In order to contribute to further understanding of the dynamic of the Madeira Island wake, in the follow-up of Caldeira et al. (2002), the objectives proposed herein are to (a) study the asymmetry of the near-field wake; in other words, study island-induced structures in the early stages of their life-cycles (near the island, 1-2L); (b) to study the roles of the nearest neighboring islands (Desertas and Porto Santo); and (c) study the role of the island-shelf in the modulation of vortex shedding.

After this introduction, the paper comprises a section briefly discussing the regional oceanographic setting and therefore exposing the motivations behind the choices made during the setup of the experiments. Thereafter, there is a detailed description of the model used and of the experimental setup, followed by the results and discussion section. In the summary and conclusions section, the main results are highlighted, including some suggestions for further work.

2 Oceanographic setting

Madeira is an archipelago located in the Northeast Atlantic (32.5° N; 17° W). The archipelago has several sub-groups of islands: Madeira and Porto Santo are inhabited, whereas Desertas and Selvage Islands are uninhabited, natural reserves. In this study, the influence of neighboring islands (Desertas and Porto Santo) was considered due to its close proximity to Madeira, i.e., 20–40 km (Fig. 1).

There are few oceanographic studies attempting to characterize the Madeira regional oceanographic setting, and in situ data are scarce. Caldeira et al. (2002) presented a first attempt at identifying the dominant ocean scenarios for the region, but at that time, only passive satellite data were used. Passive satellite data, namely thermal and color data, from Advanced Very High Resolution Radiometer, from Sea-viewing Wide Field-of-view Sensor, or from Moderate resolution Imaging Spectroradiometer (MODIS), satellites are limited by clouds and therefore it is hard to follow the time and spatial evolution of oceanic structures, in particular over the deep ocean, with high evaporation rates. Most recently, merged datasets try to overcome the spatial limitations caused by cloud coverage, however compromising the ability to resolve synoptic events, since merged products average conditions during several days, weeks, or months. Altimetry-derived products are not limited by clouds, but it

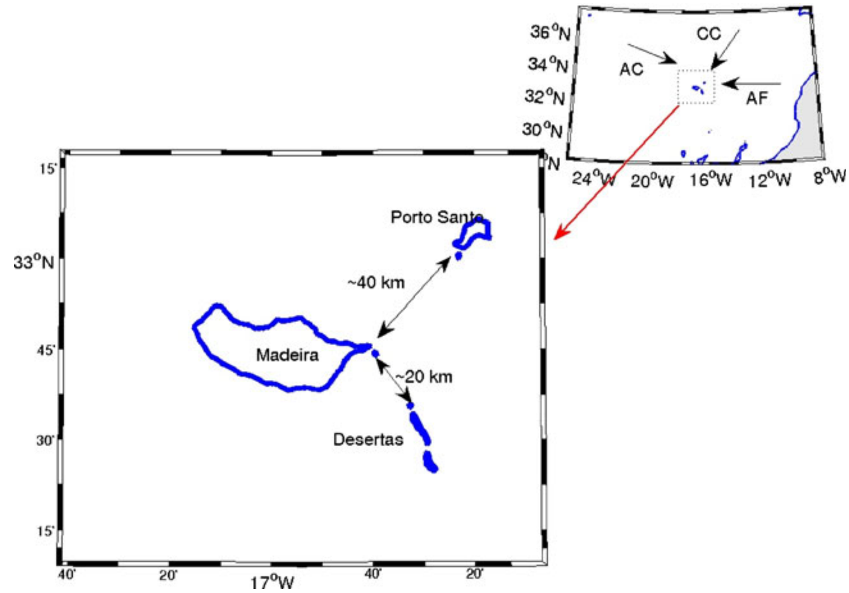

Fig. 1 Map of the Madeira Archipelago showing the location of the main islands (Madeira, Desertas, and Porto Santo) and the relative distances between them; the direction of the ocean surface currents affecting the archipelago are also indicated: *AC* Azores Current, *CC* Canary Current, *AF* African filament

has only recently become possible to combine data from several altimetry satellites in order to achieve an adequate spatial resolution to study the variability of mesoscale phenomena. Nevertheless, altimetry data processing is very sensitive to land/coast contamination preventing the accurate detection of the early stages of island-induced features, which occur in the near-field. Furthermore, altimetry products have an inadequate resolution to resolve near-field submesoscale phenomena, i.e., $<<R_{\mathrm{d}} = NH/f$ (parameters defined in Section 3.2).

In the context of very little data available due to cloud coverage affecting passive sensor products and inadequate spatial and/or temporal resolution altimetry-derived products, numerical and/or experimental models become good candidates to contribute to advancing the knowledge of the dynamics of complex wakes, such as the ones induced by multiple island arrangements (archipelagos). Following Caldeira et al. (2002) first suggestions, the working hypothesis was that Madeira Island interacted with incoming flow and induced the formation of leeward eddies. Figure 1 shows the main surface currents affecting the archipelago. Notwithstanding the historical descriptions, Caldeira et al. (2002) observed a westerly incoming flow and hypothesized this to be the influence of the Azores Current. This western inflow affecting Madeira was previously suggested to be the southern limit of the NE Atlantic sub-tropical front (Siedler et al. 1985). Although not yet considered, similarly to what occurs at the Canaries (Aristegui et al. 1997), African filaments are known to travel offshore, and occasionally, they might reach Madeira; hence, a westward flow was also considered. A southerly incoming flow, particularly at the surface, was never accounted for this region until very recently. During 2008 and 2009 oceanographic cruises, eddies were observed (using satellite and in situ data) attached and shedding from the northern side of Madeira Island; hence, a southerly incoming flow, perhaps dominated by persistent southern wind episodes, was also examined.

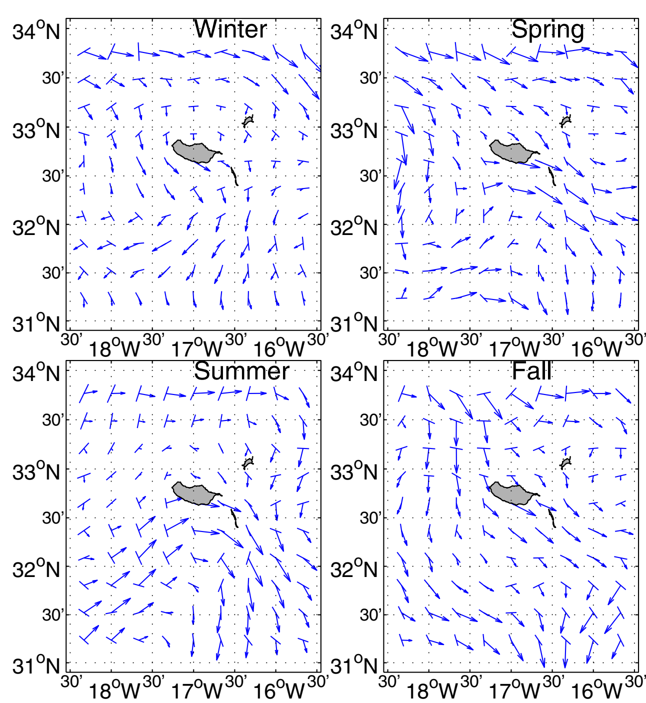

Fig. 2 Mean seasonal geostrophic currents calculated from AVISO, considering data from October 1992 to March 2010

Figure 2 shows the seasonal patterns of geostrophic currents for the Madeira archipelago region. Winter and fall geostrophic currents reach the island mostly from the north, whereas during the summer, there is a strong south inflow and during spring a strong western incoming flow. These averaged geostrophic current patterns were calculated using the AVISO altimetry archive regular gridded data, from October 1992 to March 2010.

Figure 3 is an example of a phenomena commonly detected around Madeira, using MODIS thermal and color sensors. A cyclonic eddy southwest of Madeira Island, concurrent with the detection of a high sea surface chlorophyll concentration. In fact, analysis of historical satellite data shows a bias for the detection of cyclonic eddies, which might be related to the fact that cyclonic eddies have upwelling in their core and consequently cold water reaching the surface, contrasting well with the surrounding warm sea surface temperatures (SST), whereas anticyclonic eddies have downwelling in their core and therefore they might be masked by SST from the surrounding water. Alternatively, cyclones might occur in greater numbers and/or last longer periods, thus enabling frequent satellite detection. A third possibility is that most anticyclonic eddies, formed leeward of Madeira, have weak surface signature and/or migrate to deeper oceanic regions.

Figure 4 represents a productive cyclonic eddy forming to the north of Madeira, presumably induced by a southerly incoming current. This particular episode (7 of September 2008) was sampled during an in situ campaign, and its vertical structure will be presented in upcoming discussions. A noteworthy observation is that north wake eddies are never as large as the southern ones, presumably due to the fact that the island boundary layer is different on the west (south wake side) than it is on the east (north wake side). The north eddy was resampled 20 days later, drifting north and leaving a trail of high surface chlorophyll concentration.

African filaments, namely those formed offshore of Cape Ghir, are not frequently observed reaching Madeira, particularly considering (a) the dense cloud coverage that often affects the whole region and (b) the hypothesized dominance of the Canary Current system, which is expected to induce a predominantly southward net transport. Nevertheless, September 2010 was a particularly favorable month for the occurrence of a West African filament. Figure 5 shows the trail of sea surface chlorophyll concentration (apparently) brought via a coastal filament episode, reaching Madeira from the east. Data represent a monthly, 9-km averaged sea surface chlorophyll, derived from the MODIS-AQUA satellite sensor. An offshore projection of the filament

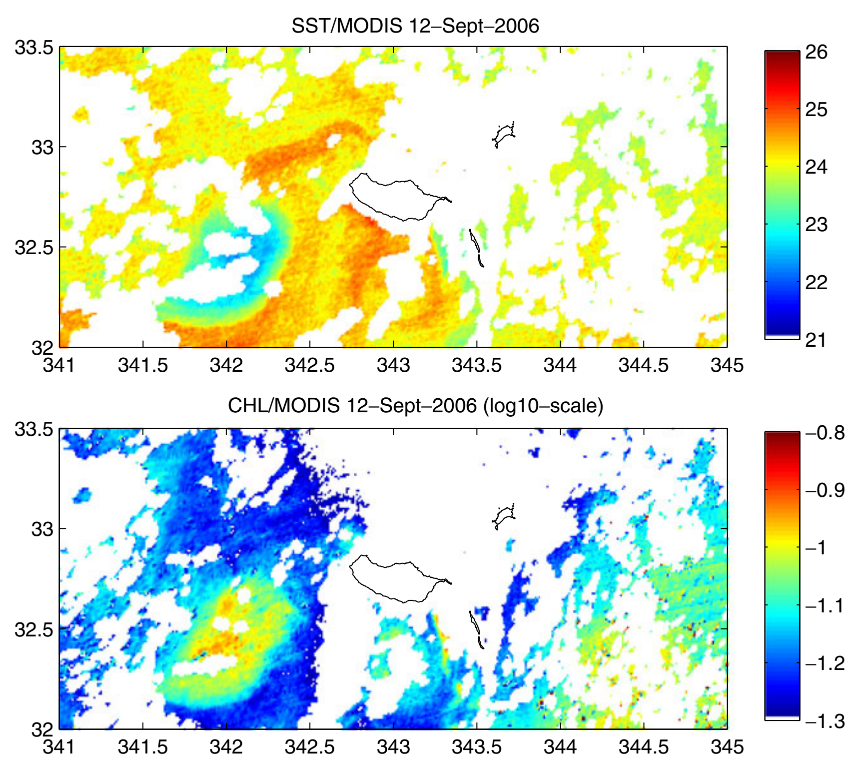

Fig. 3 Cold and productive cyclonic eddies are often detected southwest of Madeira; *top panel* sea surface temperature (°C); *bottom panel* sea surface chlorophyl (log scale). Data extracted from MODIS for the 12th September 2006 (preprocessed level 2)

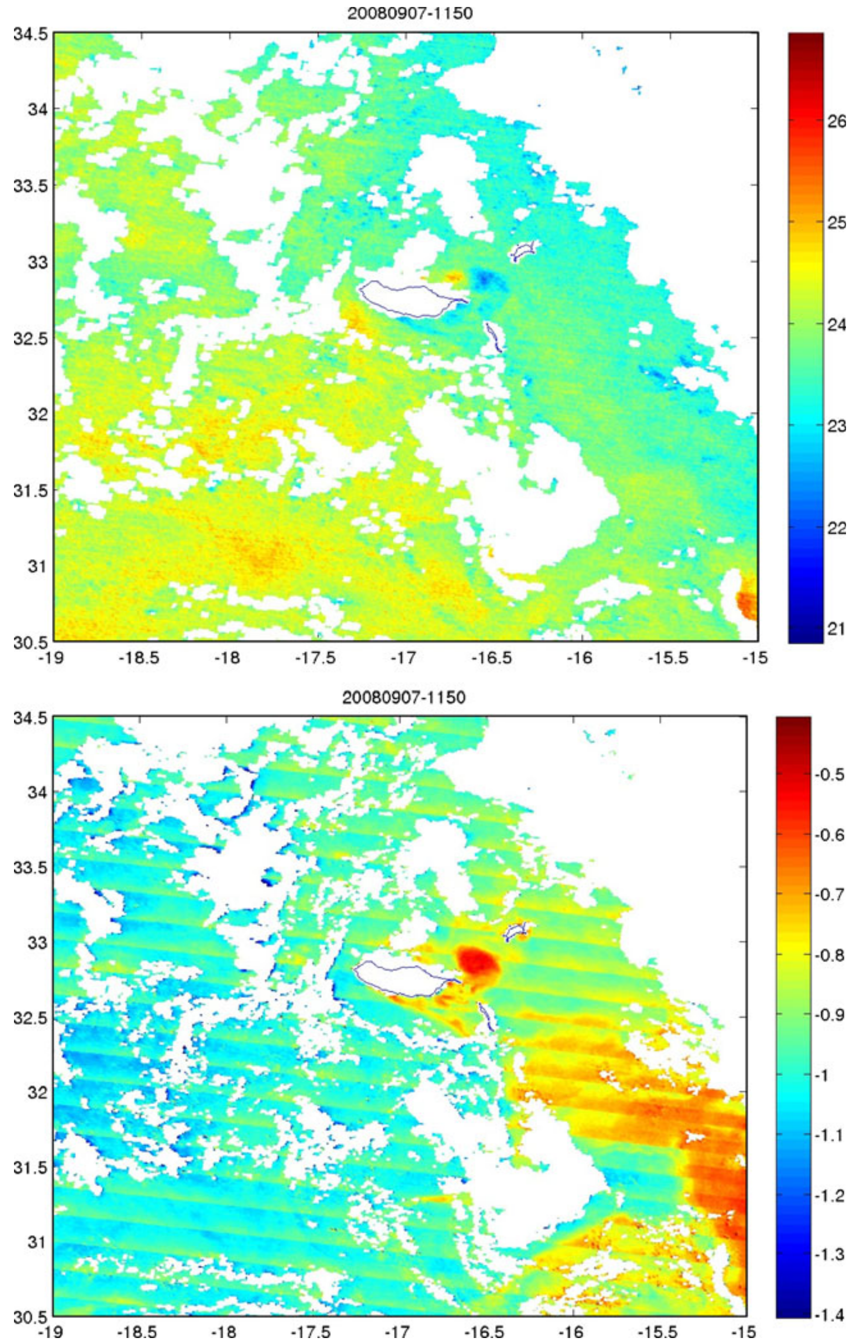

Fig. 4 Cold and productive cyclonic eddies forming north of Madeira are occasionally detected; *top panel* sea surface temperature (°C); *bottom panel* sea surface chlorophyll (log scale). Data extracted from MODIS for the 7th September 2008 (preprocessed level 2)

curls in a northwest direction; a parallel trail is also visible leeward (north) of the Desertas Islands, suggesting an incoming flow from the southeast, i.e., westward wake.

3 Numerical model

The Regional Ocean Modeling System (ROMS) was used as a full primitive equation model, to study the structure of multiple islands wakes. Since not much has been reported on complex geophysical wakes in stratified flows, the experimental setup represents a simplified version of reality, with the intent of guiding future studies. The simplifications included the elimination of possible interferences induced by neighboring seamounts and on the consideration of schematic stratification and incoming flow conditions.

3.1 The Regional Ocean Modeling System

ROMS is a free-surface, terrain-following, primitive equations ocean circulation model. ROMS algorithms

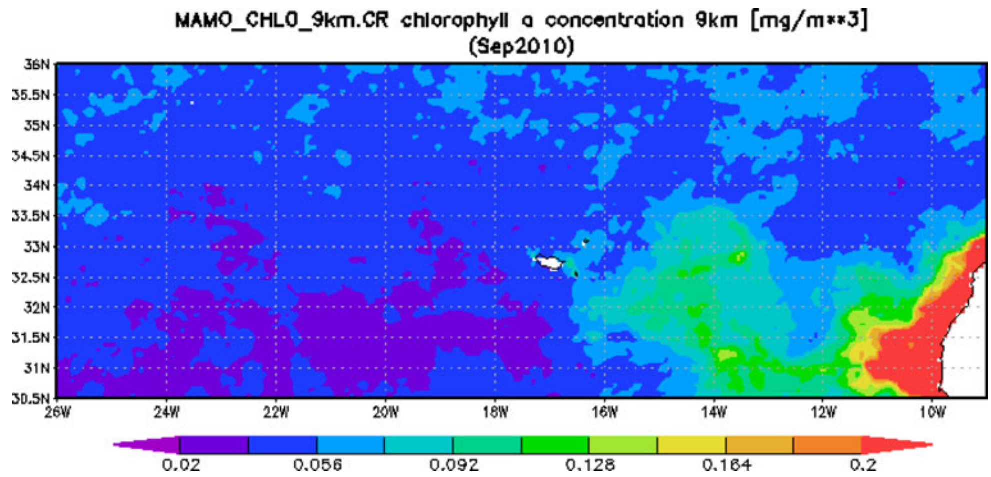

Fig. 5 Sea surface chlorophyll concentration showing the signature of an West African productive filament reaching Madeira, from the west. Data extracted from MODIS-Aqua. Monthly mean for September 2010 (preprocessed level 3 data at 9 km resolution)

are detailed in Shchepetkin and McWilliams (2003) and in Shchepetkin and McWilliams (2005). The hydrostatic primitive equations for momentum are solved using a split-explicit time-stepping scheme. A cosine-shape time filter, centered at the new time level, is used for the averaging of the barotropic fields (Shchepetkin and McWilliams 2005). Time-discretized uses a third-order accurate predictor (Leap-Frog) and corrector (Adams–Molton) time-stepping algorithm. A third-order upstream biased was used for advection in order to allow for the generation of steep gradients in the solution (Shchepetkin and McWilliams 1998). A K-profile parameterization boundary layer scheme parameterizes the sub-grid vertical mixing processes (Large et al. 1994). ROMS has been intensively used to study island wake phenomena (e.g., Dong et al. 2007; Dong and McWilliams 2007; Calil et al. 2008; Estrade and Middleton 2010; Kersale et al. 2011).

3.2 Experimental settings

A geostrophic balanced three-dimensional channel was built using a methodology similar to Dong et al. (2007). Nevertheless, unlike Dong et al. (2007), the schematic bathymetry was not an idealized cylinder with vertical side walls, but it represented the three main islands of Madeira Archipelago, including their attached shelves (Fig. 6). Data from the General Bathymetric Chart of

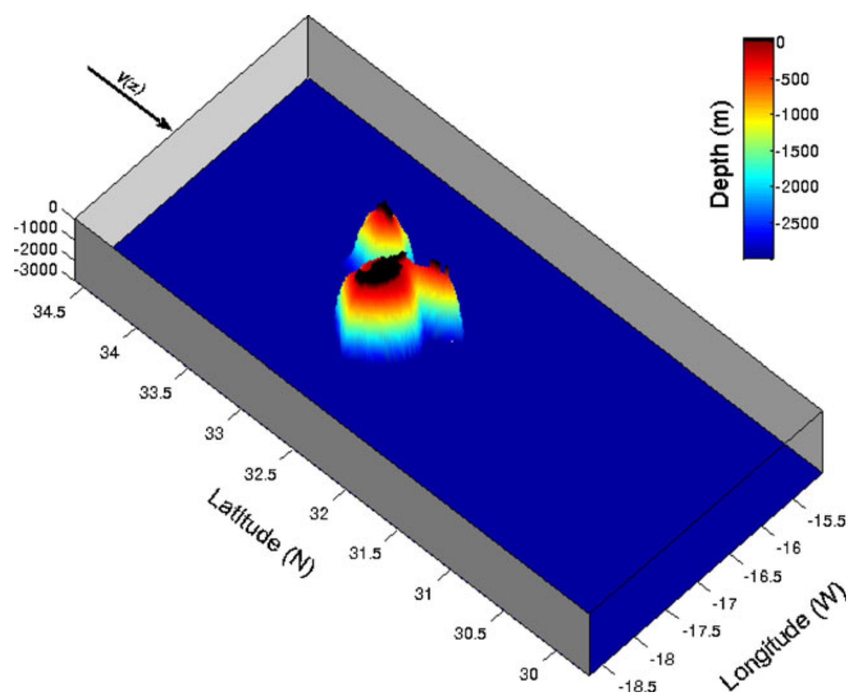

Fig. 6 ROMS numerical domain. GEBCO bathymetry data were used to generate a realistic representation of Madeira Archipelago for the ROMS study. Maximum channel depth considered was 3,000 m (*deep blue*). Other regional features such as seamounts were filtered out

the Oceans (GEBCO) were kept realistic around the islands down to 3,000 m maximum depth. All other regional bathymetric features such as seamounts were filtered out. The Madeira Island platform was centered in a channel-like configuration with a prescribed inflow at the upstream boundary such that the zonal current depended only on the vertical shear. East and west channel boundaries were set to slippery-tangential with zero normal conditions, whereas boundaries around the island were set to zero-normal and no-slip conditions. At the southern open boundary, a clamped condition was used for density in order to maintain geostrophic stability, and radiation conditions were used for momentum associated variables, warranting clean outgoing baroclinic flows, i.e., virtually free of internal wave reflections. A numerical sponge was also applied upstream of the southern open boundary, where viscosity and diffusivity incremented linearly (50–600 $m^2\ s^{-1}$) over the last 5% of the model domain. At the bottom, the quadratic bottom friction law was applied. Initial conditions were set equal to the inflow conditions in the interior domain, except at the E–W channel walls and at the island boundary points. To maintain geostrophic equilibrium in interior of the domain, the following assumptions were made.

The initial and northern boundary velocity profiles were taken as:

$$v(z) = \frac{c_1}{2}\left[1 + \tanh\left(\frac{z + h_s}{h_d}\right)\right]. \quad (1)$$

Considering the thermal wind balance, density field is constant in y-direction and can be written as a function of x and z:

$$\rho(x, z) = \rho_0 + h(z) - \frac{\rho_0 f}{g}\int_{x_m}^{x}\frac{\partial v}{\partial z}dx. \quad (2)$$

Density anomaly $h(z)$ can be taken as:

$$h(z) = \delta_\rho \tanh\left(\frac{z + h_c}{h_t}\right). \quad (3)$$

Considering the linear equation of state, neglecting salinity:

$$\rho = \rho_0 - \rho_0 c_T(T - T_0). \quad (4)$$

Temperature can be written as:

$$T(x, z) = \frac{1}{c_T} - \frac{\rho}{\rho_0 c_T} + T_0. \quad (5)$$

A linear function was used for free surface:

$$\zeta(x) = \frac{c_1 f}{g}(x - 2x_m). \quad (6)$$

where:

Symbol	Description	Units
h_s	central depth of shear layer	meters
h_d	thickness of shear layer	meters
c_1	near-surface v-velocity component	meters per second
h_c	central depth of thermocline	meters
h_t	thickness of thermocline	meters
f	Coriolis-constant	1 s^{-1}
c_T	coefficient in linear equation of state	per degree Celsius
ρ_0	mean density	kilograms per cubic meter
T_0	mean temperature	degree Celsius
δ_ρ	half of (approximate) density difference between bottom and surface	kilograms per cubic meter
x_m	middle of domain in east–west direction	meters

In the Madeira Archipelago case study, U (c_1) in Eq. 1 assumed a maximum value at the surface. In order to vary Reynolds ($Re = \frac{UL}{A_H}$), horizontal viscosity A_H, represented by the Austausch coefficient, was adjusted, considering U—the incoming flow which was maximum velocity at the surface and L—the island and/or archipelago width. Viscosity is calculated explicitly in ROMS; therefore, it can be set to zero without excessive computational noise or instability (refer to discussion in Dong et al. (2007), Section 2.2). The geostrophic channel was represented on a regular grid 221×351 grid-points (with $\delta x = \delta y \sim 1.5$ km). In sigma coordinate models such as ROMS, the bathymetry still needs smoothing and the slope parameter ($r = \Delta h/h$) was kept under 0.2 (Beckmann and Haidvogel 1993). To preserve sufficient resolution in the upper ocean, 30 vertical levels were considered. The velocity in Eq. 1 and temperatures profiles (Fig. 7) assumed the following parametrization: $\rho_0 = 1{,}027$ kg m^{-3}, $T_0 = 10°C$, $c_T = 1.7^{-4}$, and $g = 9.81$ ms^{-1}. The model was integrated for 150 days, considering a representative but constant f throughout the whole channel (9×10^{-5}), i.e., no β effect. The parameters were adjusted in order to keep all experiments under the similar regimes; $Ro = \frac{U}{fL} \sim 0.1$, thus implying a geostrophic constrain to flow evolution. Considering the Brunt–Väisälä buoyancy frequency ($N^2 = -\frac{g}{\rho_0}\frac{\partial \rho}{\partial z} \sim 10^{-3}$) and the baroclinic deformation radius $R_d = \frac{NH}{f} \sim 40$ km, where $H \sim 10^2$ is the vertical scale set by the upstream flow and density profiles (h_d in Eq. 1), the Burger number was kept close to unity (Bu ≈ 1), considering $Bu = \left(\frac{R_d}{L}\right)^2$, in all the ROMS experiments discussed herein.

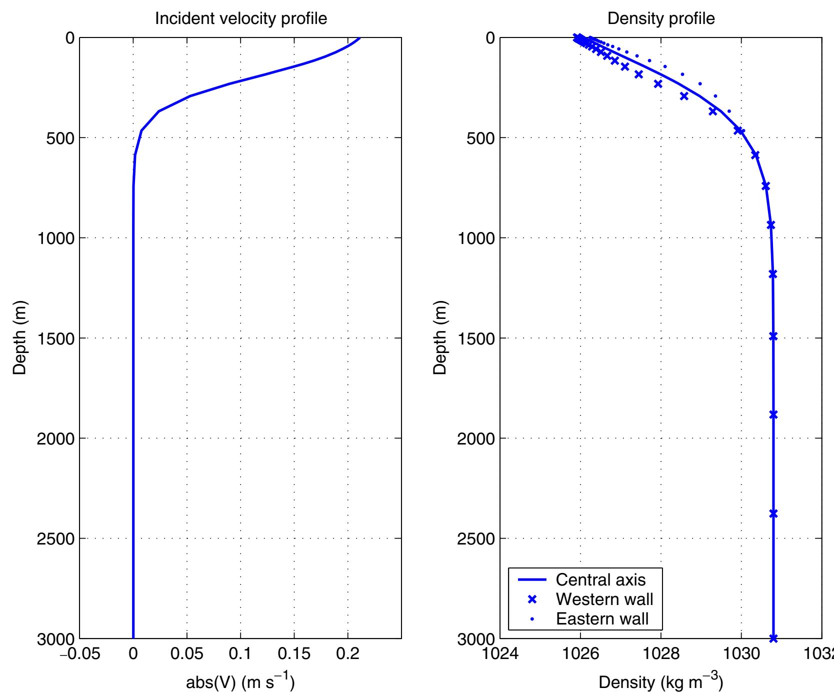

Fig. 7 ROMS initial profiles of velocity (*left panel*) and density (*right panel*) generated analytically using an hyperbolic tangent. Western and Eastern profiles needed to be adjusted according to the thermal wind balance relationship. Position of the vertical gradients are representative of the regional pycnoclines. Daily and seasonal variations were not considered in this study

4 Results and discussion

Dong et al. (2007) used ROMS to study the different regimes in a deep-ocean wake condition. Considering the role of stratification and planetary vorticity, the authors concluded that as Bu decreased, the eddy size shrank from being close to the island width (L) and to the baroclinic deformation radius, and thus, the eddy generation process shifted from barotropic to baroclinic instability. Furthermore, for small Ro values, the wake was symmetric with respect to cyclonic and anticyclonic eddies. Another wake study of gaussian-shaped islands, taking into account a linear underwater shelf, was pursued by Dietrich et al. (1996). Results suggested that the presence of a shelf in a stratified deep-oceanic condition did not affect the geometry of the wake eddies but lead to a 67% increase in eddy shedding. Dietrich et al. (1996), Dong et al. (2007) are therefore strongly recommended complementary readings. In the Madeira wake study, due to its asymmetric nature and multiple island composition, changes in the incoming flow direction needed careful consideration.

4.1 Direction of the incoming flow

Considering that Madeira Island irregular shape has different wake responses, when compared to symmetrical obstacles, it is necessary to also consider the different boundary layer responses induced by the four main incoming flows. As discussed in Section 2, the choices of inflow directions mimic identified oceanographic scenarios for the region which include but are not be limited to: (a) a Canary, north incoming current; (b) a South incoming current; (c) an Azores, western incoming current; and (d) an African filament, a westward penetrating flow.

4.1.1 North and south

Fully developed wakes are formed, considering a north incoming flow (Fig. 8), for moderate ($Re = 500$) and very high Reynolds ($Re = 1500$). Madeira (one-island) case generates an asymmetric wake, with strong positive vorticity (west flank) contrasting with very week negative vortices at the surface (east flank). The introduction of the other two-island groups continued to favor cyclonic eddy formation, although the small islands (Desertas and Porto Santo) contributed significantly to small anticyclonic vorticity generation at the surface. Nevertheless, the introduction of the neighboring islands manifestly disrupted the wake formation. As can be seen in Fig. 8, small patches of negative vorticity reach the western flank, clearly affecting the western (positive) boundary layer. Comparatively, the one-island case generates much stronger cyclones, represented by stronger and larger cores, in relation to the archipelago case.

Analyzing the wake vertical structure vorticity is well represented down to 500 m (see Fig. 9); 500 m is also the bottom of the prescribed pycnocline and

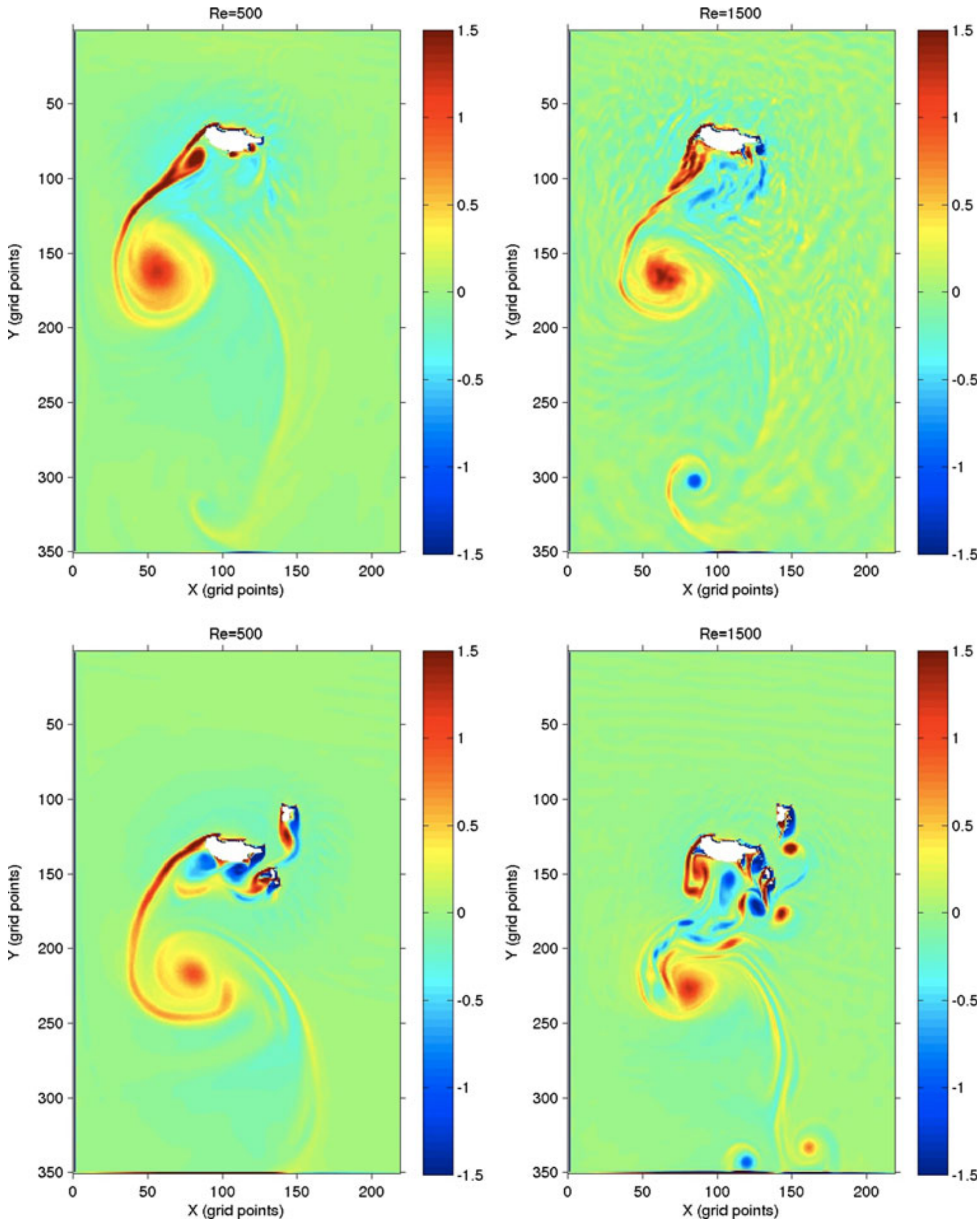

Fig. 8 Vorticity outputs from the three-dimensional ROMS study, after 30 days of computation; *top panels* represent one island case; *bottom panels* represent the archipelago case; *left panels* are for the moderate ($Re = 500$) case; *right panels* represent the results for the high ($Re = 1{,}500$), case studies

below which the velocity is null, i.e., top layer in the stratified channel. The cyclonic eddy weakens with depth, loosing its integrity at around 200 m (edge of the island continental shelf). On the other hand, the anticyclonic circulation gains momentum with depth; negative vorticity assumes a different behavior below 300 m (Fig. 9). At 500 m, the anticyclonic vorticity is the strongest and contained within a cyclonic rim around the archipelago. Below 500 m, vorticity is lost, reaching negligible values thereafter. The introduction of the neighboring islands (Desertas and Porto Santo) changes the wake scenario; cyclonic and anticyclonic vorticity formations are weaken (Fig. 10). At 500 m depth, positive vorticity is advected onto the anticyclonic vorticity rim; in fact, all the wake generated by the presence of Porto Santo is also advected onto the Madeira rim circulation. Small eddy contributions shed away, down to a depth of 200 m; thereafter, between 300 and 500 m, vortices are contained within the anticyclonic circulation and do not shed. Comparatively to the one-island case, the archipelago generates smaller but more patches of negative vorticity at the surface (0–200 m), which act to disrupt more efficiently the activity in the cyclonic boundary layer as well as to an overall weakening of the anticyclonic regime surrounding the archipelago (around the 500 m isobath).

In the south incoming flow case (Fig. 11), weaker cyclones are generated on the eastern side of Madeira,

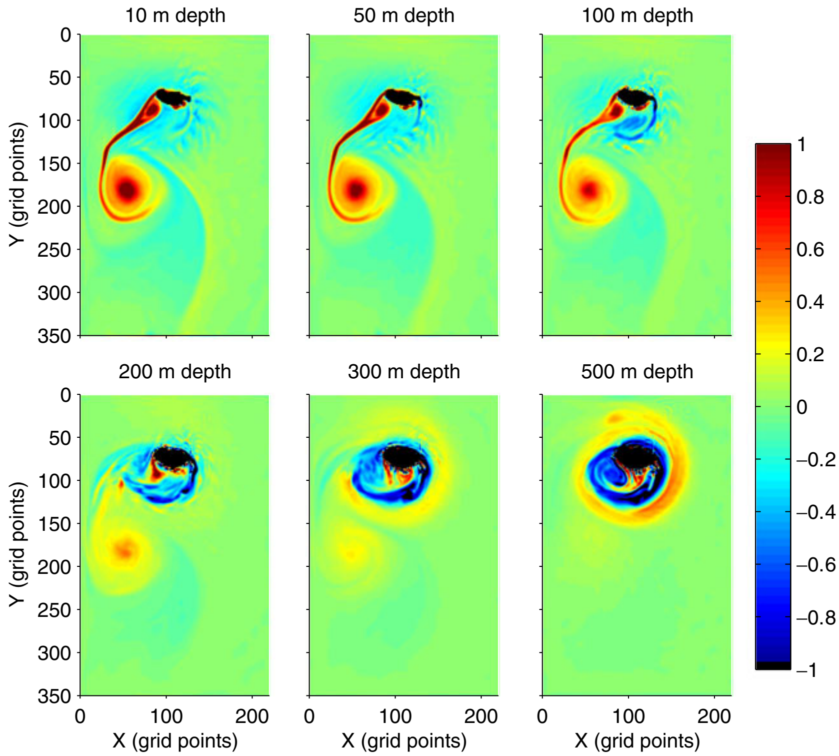

Fig. 9 Depth distribution of vorticity for the previously mentioned north one-island incoming flow (*top-panels* of Fig. 8); from the three-dimensional ROMS study, after 30 days of computation; considering a moderate ($Re = 500$) case

with a strong contribution of cyclones generated by the neighboring island of Porto Santo. The Madeira eastern boundary layer is strongly affected by the presence of Desertas. Considering that Porto Santo is less than half the size of Madeira, the cyclones generated to the north are smaller and weaker than the cyclones generated to the south. The anticyclonic vorticity generation is also weaker, constraining the advection of a cyclonic

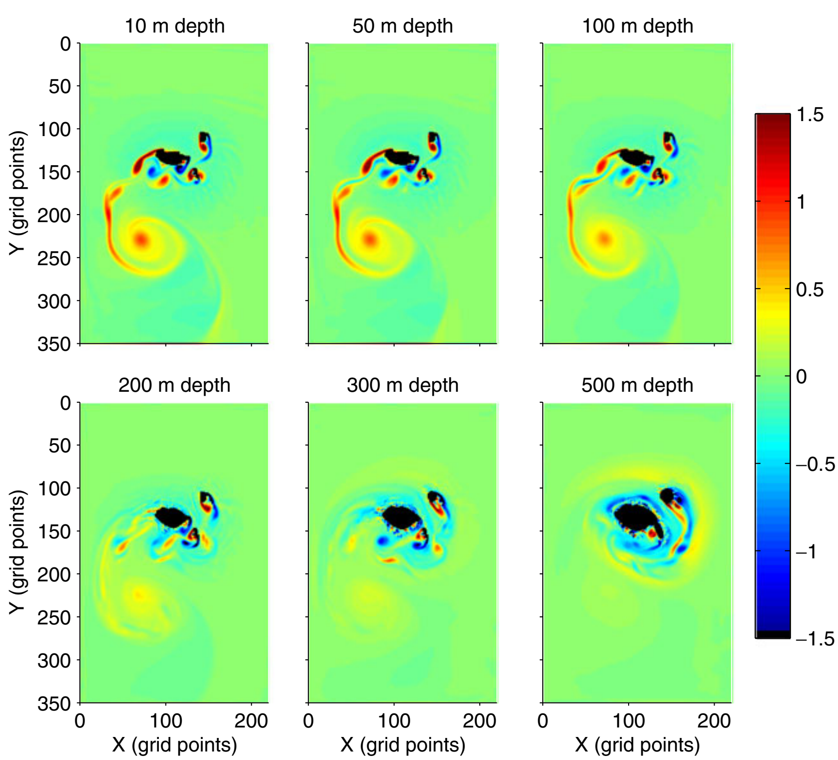

Fig. 10 Depth distribution of vorticity for the previously mentioned north incoming flow affecting the archipelago (*bottom panels* of Fig. 8); from the three-dimensional ROMS study, after 30 days of computation; considering a moderate ($Re = 500$) case

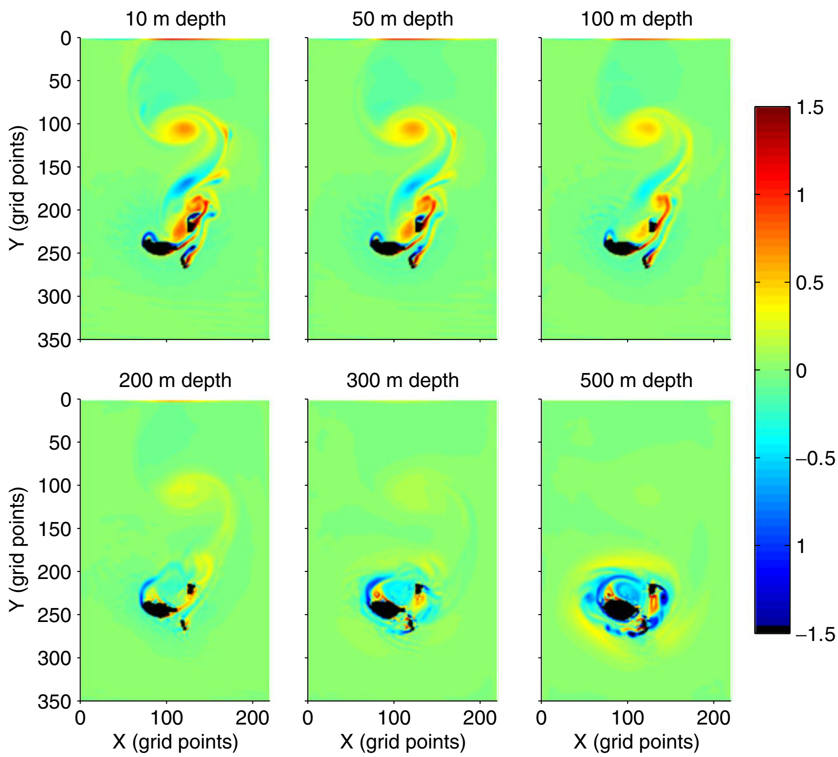

Fig. 11 Depth distribution of vorticity, considering a south incoming flow affecting the archipelago; from the three-dimensional ROMS study, after 30 days of computation; considering a moderate ($Re = 500$) case

rim at 500 m. These differences between northern and southern wakes have also been observed with satellite imagery (see discussion on north wake eddy in Section 2); northern cyclonic eddies are often observed as weaker and smaller when compared to southern ones.

4.1.2 West and east

The island encountered on the east–west perspective is very differently shaped from the island encountered from the north–south perspective; the first and most obvious difference is the island width (L); the island width orthogonal to the incoming flow is halved, considering the east–west perspective. Therefore, eddies formed from the east–west perspective are expected to be approximately half the size of the eddies considering a north–south perspective. Therefore, the change in eddies size from mesoscale ($\geq R_{\mathrm{d}}$), to submesoscale ($< R_{\mathrm{d}}$), also mean a change in the planetary scales influencing the eddy behavior from geostrophic to ageostrophic dynamics.

The studied (W–E) scenarios also considered fully formed Karman streets ($Re = 500$), although with very different outcomes, when compared to the north–south cases. Cyclones are rounder in the eastward wake (flow from the west; Fig. 12), whereas they assume an elliptical shape in the westward wake (flow from the east; Fig. 13). There are more individual eddies generated for a eastward wake, than there are for a westward one; the eastward wake is also less perturbed by the neighboring islands of Desertas and Porto Santo, located leeward of the incoming flow and leeward of the main island (Madeira). In both (W–E) cases, trapping of anticyclonic circulation around the island is also weaker comparatively to the former case study. This difference between W and E wakes is well depicted in the mean velocity profiles of the wakes. Figure 14 represents the mean velocity profiles over one shedding period, for the eastward and westward wake cases. The profile representative of the eastward wake is approximately gaussian-shaped, whereas the profile representative of the westward wake is noisier, suggesting a stronger near-field flow perturbation.

Another noteworthy result is that near-field vorticity is flushed away in a wave-like motion. Shed submesoscale eddies also loose their energy faster when compared to the N–S case. Considering its smaller size and duration, it is therefore understandable that eddies generated by W–E incoming flow regimes are not as easily detectable by satellite sensors. Land-contamination and/or limited pixel resolution often limits sensors from adequately resolving submesoscale features.

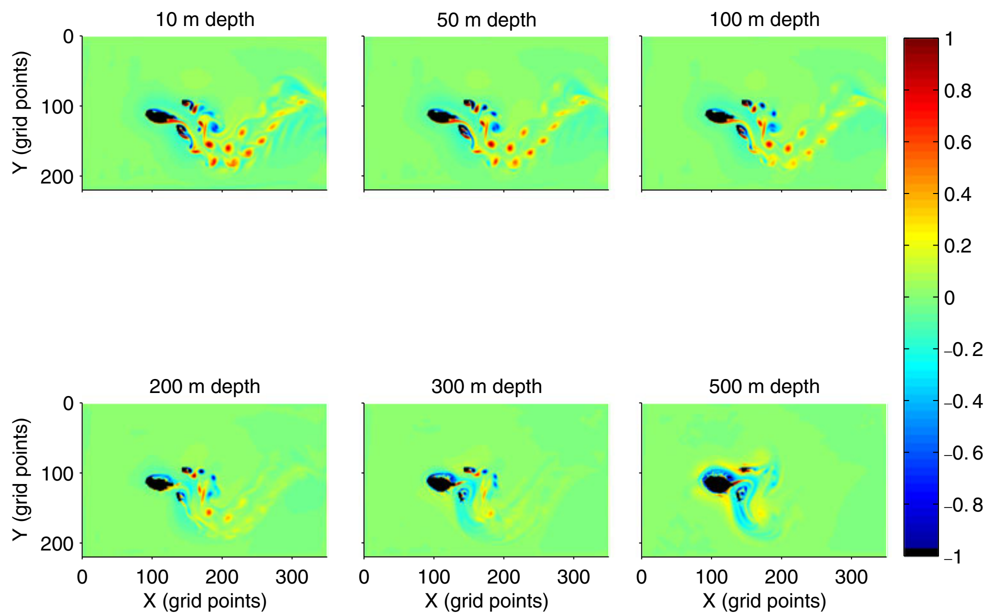

Fig. 12 Depth distribution of vorticity, considering a west incoming flow affecting the archipelago; from the three-dimensional ROMS study, after 30 days of computation; considering a moderate ($Re = 500$) case

4.2 "Flapping wakes"

An archetype of a wavy-wake is produced by the flapping of a flag. Zhang et al. (2000) used experimental foaming films to study the physics of filament wake structures, whereas rigid filaments induced the formation of a narrow Von Karman Vortex street, composed of eddies of alternating sign, similar to those produced by small cylinders. On flapping, filamental structures formed a street of small eddies of a single sign arranged in a wave-like pattern. These flapping wakes resembled the outcome from a Kelvin–Helmholtz instability; nevertheless, the resulting vortical field does not develop eddies of a size comparable to the flapping amplitude, but significantly smaller. Of course in the Madeira wake study, the islands were not moving targets, but the coastal trapped waves generation mimicked the flapping of flag, thus creating a qualitatively similar effect (see on discussion coastal trapped waves in Section 4.4).

Another known characteristic of flapping wakes is the inverted hydrodynamic drafting effect (e.g., Ristroph and Zhang 2008; Alben 2009). In tandem experiments, inverted drafting suggested that each flag

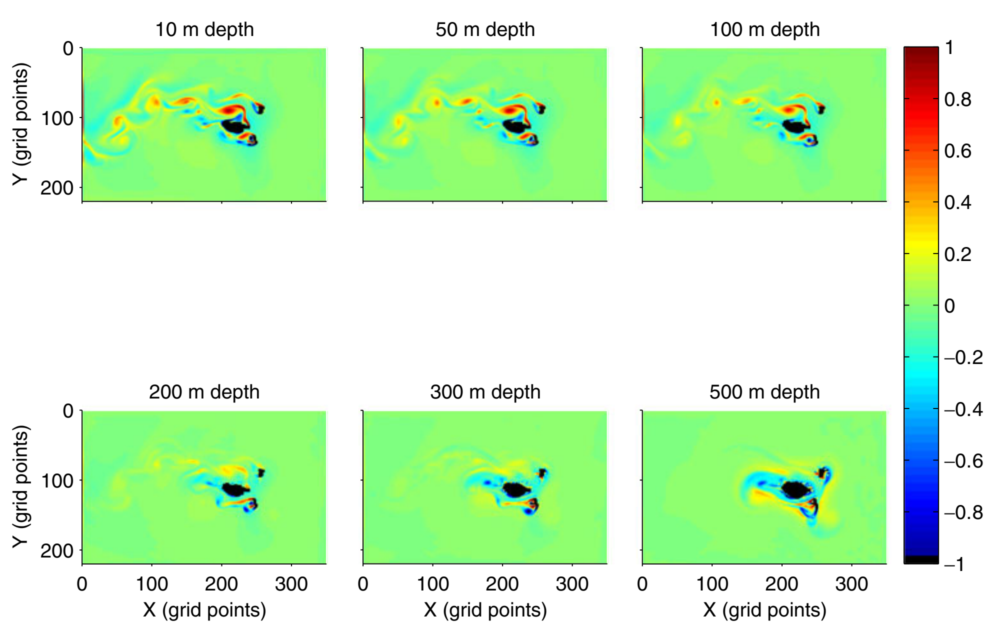

Fig. 13 Depth distribution of vorticity, considering a east incoming flow affecting the archipelago; from the three-dimensional ROMS study, after 30 days of computation; considering a moderate ($Re = 500$) case

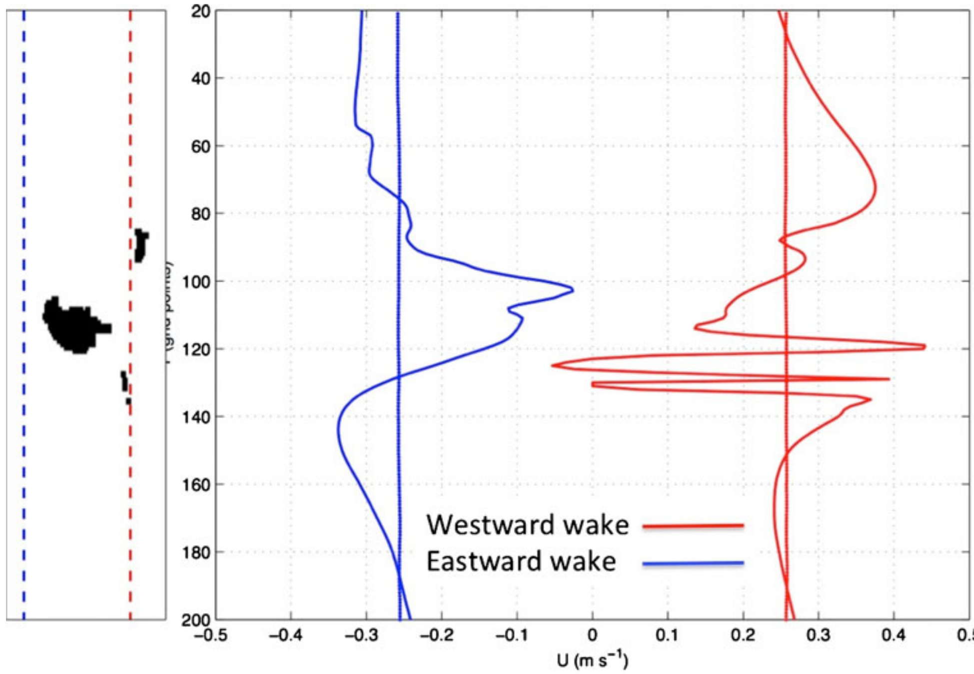

Fig. 14 Comparison between mean surface velocity profiles for the **a** westward wake (*red line*—flow from the east, Fig. 13) and **b** eastward wake (*blue line*—flow from the west, Fig. 12) for the $Re = 500$ case studies; *straight lines* represent (unperturbed) windward profiles (before the island)

modifies its surrounding flow introducing changes in the form of motion to the other flag (e.g., Ristroph and Zhang 2008). When the flags are sufficiently close, the leeward flag undulates in the oscillating frequency of the windward flag. This synchronized wake oscillation creates a counter-intuitive resonance effect, resulting in higher drag for the leeward flag (e.g., Ristroph and Zhang 2008; Alben 2009). Analogously, in the Madeira case study, the W–E wake is mainly controlled by the leeward islands. In the eastward wake case, Desertas and Porto Santo are responsible for the generation of most ageostrophic eddies, whereas in the westward case, Madeira Island takes the increase drag role and consequently induces the formation of larger yet fewer elliptical eddies, leeward of the small islands.

Thus far, the flapping-wake phenomena had only been captured in two-dimensional studies and exclusively for non-rigid bodies. To the best of our knowledge, this is the first documented occurrence for a geophysical, three-dimensional stratified flow configuration, involving a rigid obstacle.

4.3 Multiple-islands effects

Vortex shedding behind circular cylinders can be altered or even suppressed by the proper placement of a "control cylinder" in the near-field of the main cylinder. Such phenomenon has been documented in several laboratory and numerical studies (e.g., Strykowski and Sreenivasan 1990; Sakamoto et al. 1991; Dalton et al. 2001). It is argued that the presence of a second obstacle has the effect of "altering the local stability of the flow by smearing and diffusing concentrated vorticity in the shear layer" (Strykowski and Sreenivasan 1990). Several hypothesis have been put forward to explain this change of stability in the shear layer, the most generally accepted one being the fact that the presence of the small cylinder alters the instability mode in the near-field region from absolute to convective. Strykowski and Sreenivasan (1990) found that proper placement is not just on the wake side of the main cylinder but on the shear-layer region (an elliptical region leeward and side ways the main cylinder, illustrated by Fig. 20 in Strykowski and Sreenivasan (1990)). In the N–S study case, Desertas near-field positioning is within the shear-layer region of Madeira ($l/L = 2.5$; $y/L = x/L = 0.6$, where l—width of the small island Desertas, L—width of the larger island Madeira, and y/L and x/L—the positioning of the small island relatively to the large one, considering the origin point (x_0, y_0), to be the center of the larger island). Although Madeira, Desertas, and Porto Santo Islands cannot be considered cylinders, some analogous interpretations can be made.

The wake profiles shown in Fig. 15 represent a southward wake (north incoming flow), and the windward (green) line represents the averaged unperturbed incoming flow, whereas the profile extracted leeward of the island (black line) captures the island-induced wake. The mean velocity profile generated after one

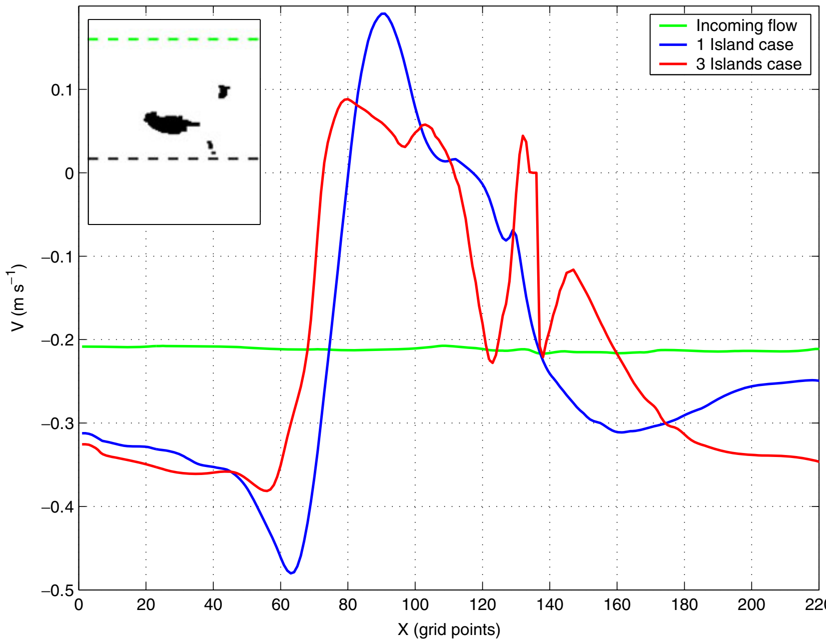

Fig. 15 Mean surface velocity profiles before (*green*) and after the island, showing the wake signal of **a** Madeira Island (*blue*, Fig. 8, *upper panel*); and **b** Madeira Archipelago (*red*, Fig. 8, *lower panel*)

shedding period for the one island case is substantially different from the three-island (archipelago) case. The one-island case represented a close to gaussian-shaped wake profile, whereas the archipelago case becomes bimodal. Bimodal profiles are symptomatic of the near-field disruption by the neighboring Desertas Islands.

In spite of the fact that previous control-cylinder experiments have only considered 2D barotropic flows, Protas (2008) anticipated that if such 3D vortex models could be established, they would be amenable to treatment using control methods analogous to those described in the context of two-dimensional cases. In fact, results from the Madeira wake studies suggests that neighboring islands continue to disrupt the near-field boundary layer stability, weakening the overall vorticity generation. In the N–S case study, Desertas and Porto Santo induced the generation of submesoscale vorticity, which was advected onto larger mesoscale cyclones, contributing to its destabilization and subsequent loss of vorticity. On the other hand, when considering a W–E incoming flow, all islands were of approximately the same size (L) and thus the combined Karman street organized itself on a wave-like pattern, under the control of flapping wake dynamics (discussed in Section 4.1.2). In summary, Madeira Island case studies leads to speculate that perturbed wakes composed by eddies of the same order of magnitude and, in phase, do not disrupt the same way as wake systems composed by different size eddies. In fact, Sangra et al. (2005) in their study of time and spatial evolution of an island-induced mesoscale anticyclonic eddy showed that eddy merging is favored for eddies with approximately the same size and rotation, whereas eddies of different sizes and/or of different rotation signs need several interactions, exhibiting some initial repulsion, before eventually merging. The study was based on the orbital motions of eddies observed using drifters and satellite imagery. Vortex merging discussions were substantiated with an inertial stability model. In general, eddy interaction can be considered a destabilization factor to the angular momentum.

Multiple-island systems somewhat resemble wakes induced by permeable bodies such as porous screens, walls, meshes, or even multiple disks arranged in a axisymmetric fashion. Therefore, the study of aeronautical and industrial turbulent flows through porous screens can provide important clues in the nature of complex geophysical wakes. Experimental results comparing the wakes of a circular cylinder with the wake emitted by a porous solid screen indicated that self-preservation is achieved in significantly different manners in these two cases (Antonia and Mi 1998). In the cylinder wake, the normalized Reynolds stresses and vorticity decreases continuously toward the self-preserving state, whereas the opposite is observed in the screen-induced wakes. Thus, these contrasting behaviors reflect important structural differences between the two types of wakes. The decay of the Karman vortex street dominates the near and intermediate regions of the cylinder wake. The near-field wake of a screen is dominated by the merging/pairing of the leeward vortices; however, the strength of these vortices monotonically increase with distance. Therefore, the decoupling from initial conditions occurs at a much smaller distance for the screen wake than it occurs for the cylinder wake.

Huang et al. (1995) studied the time evolution of wakes induced by a porous body and concluded that in the near-field region, the flow contained small-scale vortices in the shear layers which tended to interact and merge with each other, such as the shear layers observed in the N–S Madeira wake. This leaded Huang et al. (1995) to conclude that the flow is three-dimensional in the near-field, subsequently becoming more organized and two dimensional in the far-field. Near-field wake structures generated by a porous body are subjected to intense three-dimensional disturbances, most probably as result of the smaller scale lateral vortices (Huang et al. 1995).

The near-field disruption of the Madeira Archipelago wake was also (partially) captured during a laboratory experiment, conducted at the LEGI-Coriolis (14 m diameter) rotating table in Grenoble (France). A total of 67 experiments were conducted to study the impact of rotation and stratification on small-scale inertial instabilities. The experimental setup considered an upper thermocline layer on the top of a deep barotropic ocean. Particle image velocimetry (PIV) techniques were used to calculate the surface vector field as well as derive other related variables such as vorticity. Unfortunately, no vertical PIV characterization was carried out (refer to Perret et al. 2006; Teinturier et al. 2010, for similar laboratory setups and data processing procedures). Apart from considering the wake flows induced by different sized cylinders, the experiment was also carried in elliptical models of the Madeira and Azores Archipelagos. The experimental results discussed herein were run under the similar parameter regimes: similar stratification $14 < S(= N/f) < 20$ and the same $Re \sim 10000$ (towing velocity), where (S) is the stratification parameter, which is a function of Brunt Vaisala and the Coriolis parameter (adjusted in the laboratory with the solid body rotation of the turn table). Further analyses are being carried in order to discuss in detail the role of inertial instabilities during wake generation; nevertheless, two particular cases shown in Fig. 16 are relevant to include in the current discussion. Considering similar regimes, whereas in the cylinder, the two boundary layers had similar (near-field) behavior, in the (elliptical) Madeira–Desertas Archipelago case, the anticyclonic side (Desertas) produces independent smaller eddies, which interfered with the anticyclonic shedding. The cyclonic integrity, however, was maintained. It is hypothesized that the contribution of strong (smaller) positive vortices in the near-field of the anticyclonic side due to the presence of a small neighboring elliptical island (e.g., Desertas) played a significant role in the wake destabilization. Qualitatively the laboratory results corroborate the numerical results, shown in Figs. 8 and 10. These experiments only accounted for a north incoming flow, but future analysis will consider flows from different directions, under similar laboratory regimes.

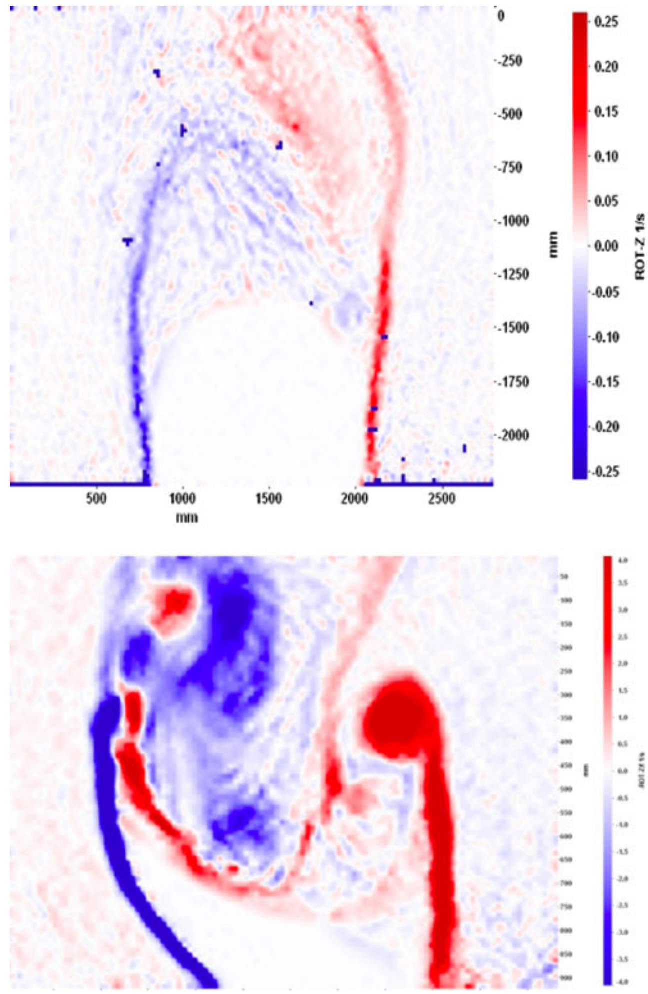

Fig. 16 Vorticity field derived from stratified laboratory experiments, comparing two geometries: cylinder (*top-panel*); two ellipses representative of the Madeira Archipelago (*bottom panel*). The ellipses and channel gaps were scaled to represent the Madeira and Desertas Islands, with *vertical side walls*, i.e., no realistic shelf effects were considered during the experiments. The near-field disruption due to the generation of submesoscale vorticity on the Desertas side is clearly visible. An animated version of the time and spatial evolution of the archipelago boundary layer can be viewed as supplementary material

Comparing the time evolution of Madeira Archipelago generated vortices (see Fig. 17), an asymmetry eddy decay was captured. Starting from

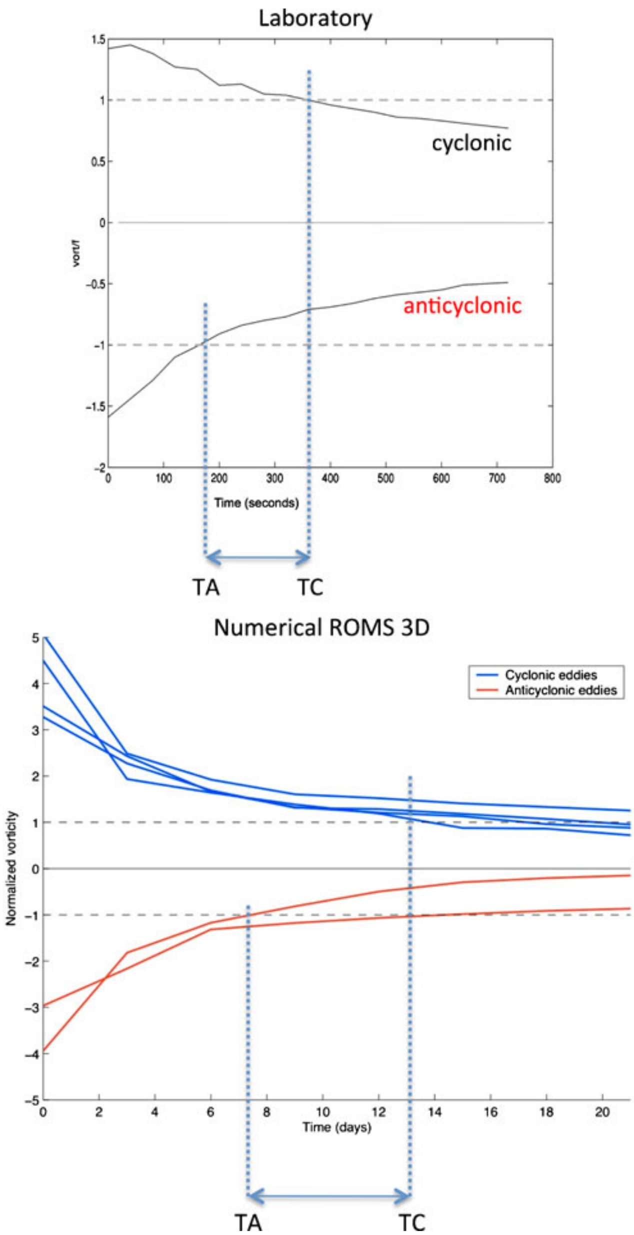

Fig. 17 Asymmetric cyclonic and anticyclonic eddy decay for the laboratory (*upper panel*) and numerical (ROMS—*bottom panel*) experiments. In both cases, anticyclones decay faster than cyclones. Multiple lines in the ROMS cases represent different *Re* parameterizations

approximately equal initial vorticity magnitudes, both anticyclonic and cyclonic vortices loose their momentum while traveling downstream, partly due to eddy viscous diffusion (Dong et al. 2007). The anticyclonic vorticity however, decays much faster than cyclonic vorticity. Dong et al. (2007) interpreted this rapid weakening of the anticyclonic wake eddies as a manifestation of centrifugal instability.

4.4 Island-shelf perturbation of baroclinic flows

The bathymetric representation of Madeira Archipelago is quite steep between 200 and 500 m (200 m being the edge of the island-self) and (close to) vertical thereafter (between 500 and 3,000 m); however, the shelf is also different in the west side (wider and smoother) when compared to the east side (steeper gradients closer to the coast). Mathematical modeling of multiscale baroclinic flows interacting with steep topography remains a challenging problem. Nevertheless, it is known that if oceanic slopes are accompanied by a steep isopycnic gradients (0–500 m), the main ingredients are meet for density-driven currents to form (e.g., Mori and Griffiths 1987; Poulin and Swaters 1999). Topographic trapped wave generation is known to result from downslope propagation of mesoscale eddies (e.g., Poulin and Swaters 1999; Sutyrin and Grimshaw 2010). In addition, off the shelf advection of eddies is also known to carry high potential vorticity (PV) offshore (e.g., Sutyrin and Grimshaw 2010). Offshore propagation of topographic waves might be responsible for the flapping-wake scenarios, whereby equivalent sized submesoscale eddies propagate offshore in a wave-like pattern, as previously discussed in Section 4.2.

There is also a different reaction documented to this PV-driven off-shelf advection mechanism; whereas cyclones that are generated by this mechanism become active components of mesoscale variability near the shelf edge, warm-core anticyclonic eddies become strongly deformed eventually resulting in their dissipation (Sutyrin and Grimshaw 2010). In the Madeira case, a combination of these mechanisms might be acting, in the presence of steep stratification and bathymetric slope gradients. Anticyclones react strongly to vertical shear instability and migrate vertically, becoming stronger at the bottom edge of the stratified layer, whereas mesoscale cyclonic eddies are stronger at the surface as they react positively to f. Holton (1992) proposed an instability criteria for baroclinic flows in which $fq < 0$, where q is the Ertel potential vorticity ($q = [f + \zeta]N^2 - \partial v/\partial z\ \partial B/\partial x$), where B is the buoyancy and ($N^2 = \partial B/\partial z$). As demonstrated by Chavanne et al. (2010), using the thermal wind balance, the following result can be obtained: ($fq = f[f + \zeta]N^2 - f^2[\partial v/\partial z]^2$); considering that in the near-field wake the flow remains inertially stable, an alternative destabilizing effect could well be a strong vertical shear (i.e., $-\ f^2[\partial v/\partial z]^2 >> f[f + \zeta]N^2$); thus, subinertial instabilities might be acting on anticyclones more efficiently. These processes should be investigate further in laboratory and numerical studies; however, hydrostatic and non-hydrostatic flows need to be concurrently resolved.

5 Summary and conclusions

To the best of our knowledge, this is the very first numerical study of the Madeira Island wake (probable) scenarios; nowhere is it suggested that all the (realistic) wake scenarios were identified. The first and foremost goal of this pioneering study is to be used as a guide for future Madeira wake studies, which should add complexity aiming at more realistic representation of the regional dynamics. Moreover, this study can also serve as a guide for future in situ oceanographic investigations. Often numerical studies either consider the very fundamental nature of wake generation (e.g., Dong et al. 2007) or the full bathymetric complexity of the studied region (e.g., Dong and McWilliams 2007; Calil et al. 2008). Nevertheless, given the limited amount of in situ data available for this region and considering satellite data limitations (e.g., open-ocean high evaporation rates, limited spatial and temporal resolutions, land contamination, etc.), it is currently impossible to validate all the wake scenarios proposed herein. Combining suggestions from previous studies of island wakes (Dietrich et al. 1996; Caldeira et al. 2002; Dong et al. 2007), with known facts from experimental fluid dynamics (e.g., Antonia and Mi 1998; Ristroph and Zhang 2008; Alben 2009), this study attempts to give insights into some of the complexity of geophysical multiple island wakes. A full primitive equation model (ROMS) was used to further explore the (a) changes in inflow directions, (b) archipelago composition, and (c) the impact of introducing an island shelf in a stratified fluid. The numerical results propose several new undocumented scenarios for the Madeira Archipelago region. The numerical representation of the circulation around Madeira Island induces asymmetry in the wake generation; this asymmetry is reinforced by the presence of the neighboring islands (Desertas and Porto Santo). Neighboring islands play an important role in destabilizing the near-field wake, with evidence of inverted hydrodynamic drafting occurring in the W–E cases. Wakes induced by north–south flows are expected to be predominantly geostrophic, generating a combination of mesoscale and submesoscale eddies, whereas west–east flapping-type wakes are expected to be predominately ageostrophic. In this context, it is not expected that E–W wake scenarios and/or the full-scope of the N–S wakes can be studied using the currently available oceanographic datasets. It is important, however, to confirm some of these dynamics by intensifying in situ data collection in the future. The island-shelf plays an important role in the dynamics of the wake generation and evolution; our results suggest that in the case of Madeira and in particular for the N–S cases, the cyclones are predominantly surface features, whereas at the bottom the first layer is dominated by an anticyclonic circulation, probably formed by downslope density currents. As suggested by former studies, inertial instabilities might strongly affect the far-field wake and the different life cycle of cyclonic versus anticyclonic wake-eddies (e.g., Perret et al. 2006; Teinturier et al. 2010); the Madeira numerical results, however, and recent HF-radar observations at Hawaii (Chavanne et al. 2010) suggest that subinertial instabilities might also be acting in the near-field, particularly around steep-island shelves.

Future studies shall continue to explore the three-dimensional aspects of the wake problem, adding more dynamics representative of region. Nevertheless, considering the non-hydrostatic nature of some inner-shelf processes, it is no less important to consider a multiscale approach in order to study the relationship occurring between near- and far-field wake dynamics. It is also expected that field observations and further analysis of laboratory studies will corroborate some of the scenarios discussed herein.

Acknowledgements The authors are grateful for research funding from FCT-Portuguese National Science Foundation. This work was initiated as part of an FCT post-doctoral grant (SFRH/BPD/14871/2003) and continued in the scope of two subsequent research funding initiatives (POCI/MAR/57265/2004; PPCDT/MAR/57265/2004). We would like to thank the contributions of Changming Dong (Charles) and Dmitri Boutov for providing some of the scripts that were used for the pre- and post-processing of the ROMS solutions. We would also like to thank Stefan Rhia and Euclides Luis for their interest in the topic; regrettably, their contribution was not eligible to be included in the current work. Discussions with Alexandre Stegner and Olivier Cadot, during Rui Caldeira's visit to the École Nationale Supérieure de Techniques Avancées (ENSTA), Paris, are reflected in the content of this report. Comments from David Dietrich and from an anonymous reviewer substantially contributed to the improvement of the first versions of this manuscript.

References

Alben S (2009) Wake-mediated synchronization and drafting in coupled flags. J Fluid Mech 641:489–496

Antonia R, Mi J (1998) Approach towards self-preservation of turbulent cylinder and screen wakes. Exp Therm Fluid Sci 17:277–284

Aristegui J, Sangra P, Hernandez-Leon S, Canton M, Hernandez-Guerra A, Kerling JL (1994) Island-induced eddies in the canary islands. Deep-Sea Res 41(10):1509–1525

Aristegui J, Tett P, Hernandez-Guerra A, Basterretxea G, Montero MF, Wild K, Sangra P, Hernandez-Leon S, Canton M, GarciaBraun JA, Pacheco M, Barton ED (1997) The influence of island-generated eddies on chlorophyll distribution: a study of mesoscale variation around gran canaria. Deep-Sea Res Part 1 Oceanogr Res Pap 44(1):71

Barton ED, Basterretxea G, Flament P, Mitchelson-Jacob EG, Jones B, Aristegui J, Herrera F (2000) Lee region of gran canaria. J Geophys Res 105:17173–17193

Beckmann A, Haidvogel D (1993) Numerical simulation of flow around a tall isolated seamount. part i: problem formulation and model accuracy. J Phys Oceanogr 23:1736–1753

Boyer DL, Davies PA (2000) Laboratory studies of orographic effects in roating and stratified flows. Annu Rev Fluid Mech 32:165–202

Caldeira RMA, Groom S, Miller P, Pilgrim D, Nezlin N (2002) Sea-surface signatures of the island mass effect phenomena around madeira island, northeast atlantic. Remote Sens Environ 80:336–360

Caldeira RMA, Marchesiello P, Nezlin NP, DiGiacomo PM, McWilliams JC (2005) Island wakes in the Southern California Bight. J Geophys Res 110:C11012

Calil PH, Richards KJ, Jia Y, Bidigare RR (2008) Eddy activity in the lee of the hawaiian islands. Deep-Sea Res Part 2 Top Stud Oceanogr 55(10–13):1179–1194. doi:10.1016/j.dsr2.2008.01.008

Chavanne C, Flament P, GurgelGurgel KW (2010) Interactions between a submesoscale anticyclonic vortex and a front. J Phys Oceanogr 40:1802–1818

Coutis PF, Middleton JH (2002) The physical and biological impact of a small island wake in the deep ocean. Deep-Sea Res Part 1 Oceanogr Res Pap 49(8):1341–1361

Dalton C, Xu Y, Owen JC (2001) The suppression of lift on a circular cylinder due to vortex shedding at moderate Reynolds numbers. J Fluids Struct 15:617–628

Dietrich DE, Bowman MJ, Lin CA, Mestas-Nunez A (1996) Numerical studies of small island wakes in the ocean. Geophys Astrophys Fluid Dyn 83:195–231

Dong CM, McWilliams JC (2007) A numerical study of island wakes in the Southern California Bight. Cont Shelf Res 27(9):1233–1248

Dong CM, McWilliams JC, Shchepetkin AF (2007) Island wakes in deep water. J Phys Oceanogr 37(4):962–981

Estrade P, Middleton JH (2010) A numerical study of island wake generated by an elliptical tidal flow. Cont Shelf Res 30:1120–1135

Furukawa K, Wolanski E (1998) Shallow-water frictional effects in island wakes. Estuar Coast Shelf Sci 46:599–608

Heywood KJ, Stevens DP, Bigg GR (1996) Eddy formation behind the tropical island of aldabra. Deep-Sea Res Part 1 Oceanogr Res Pap 43(4):555

Holton J (1992) An introduction to dynamic meteorology. Academic, New York

Huang Z, Ferre J, Kawall J, Keffer J (1995) The connection between near and far regions of the turbulent porous body wake. Exp Therm Fluid Sci 11:143–154

Kersale M, Doglioli AM, Petrenko A (2011) Sensitivity study of the generation of mesoscale eddies in a numerical model of Hawaii islands. Ocean Sci 7:277–291

Kuo CH, Chiou LC, Chen CC (2007) Wake flow pattern modified by small control cylinders at low Reynolds number. J Fluids Struct 23:938–956

Large W, Mcwilliams JC, Doney S (1994) Oceanic vertical mixing—a review and a model with no local boundary layer parameterization. Rev Geophys 32(4):363–403

Mori M, Griffiths MESRW (1987) Coherent baroclinic eddies on a sloping bottom. J Fluid Mech 183(45–62):45–62

Parezanovića V, Cadot O (2009) The impact of a local perturbation on global properties of a turbulent wake. Phys Fluids 21(071701):071701

Perret G, Stegner A, Dubos T, Chomaz JM, Farge M (2006) Stability of parallel wake flows in quasigeostrophic and frontal regimes. Phys Fluids 18(12)

Poulin FJ, Swaters GE (1999) Sub-inertial dynamics of density-driven flows in a continuously stratified fluid on a sloing bottom. II. Isolated eddies and radiating cold domes. Proc R Soc Lond 455:2305–2329

Protas B (2008) Vortex dynamics models in flow control problems. Nonlinearity 21(9):R203

Ristroph L, Zhang J (2008) Anomalous hydrodynamic drafting of interacting flapping flags. Phys Rev Lett 101(194502):1–4

Sakamoto H, Tan K, Haniu H (1991) An optimum suppression of fluid forces by controlling a shear layer separated from a square prism. J Fluids Eng 113:183–189

Sangra P, Pelegri JL, Hernandez-Guerra A, Arregui I, Martin JM, Marrero-Diaz A, Martinez A, Ratsimandresy AW, Rodriguez-Santana A (2005) Life history of an anticyclonic eddy. J Geophys Res 110:C03021

Sangra P, Auladell M, Marrero-Diaz A, Pelegri JL, Fraile-Nuez E, Rodriguez-Santana A, Martin JM, Mason E, Hernandez-Guerra A (2007) On the nature of oceanic eddies shed by the island of gran canaria. Deep-Sea Res Part 1 Oceanogr Res Pap 54(5):687–709

Shchepetkin AF, McWilliams JC (1998) Quasi-monotone advection schemes based on explicit locally adaptive dissipation. Mon Weather Rev 126:1541–1580

Shchepetkin AF, McWilliams JC (2003) A method for computing horizontal pressure-gradient force in an oceanic model with a nonaligned vertical coordinate. J Geophys Res-Oceans 108:3090

Shchepetkin AF, McWilliams JC (2005) The regional oceanic modeling system (roms): a split-explicit, free-surface, topography-following-coordinate oceanic model. Ocean Model 9(4):347–404

Siedler G, Zenk W, Emery WJ (1985) Strong current events related to a subtropical front in the northeast atlantic. J Phys Oceanogr 15:885–896

Strykowski PJ, Sreenivasan K (1990) On the formation and suppression of vortex shedding at low Reynolds numbers. J Fluid Mech 218:71–107

Sutyrin GG, Grimshaw R (2010) The long-time interaction of an eddy with shelf topography. Ocean Model 32:25–35

Teinturier S, Stegner A, Didelle H, Viboud S (2010) Small-scale instabilities of an island wake flow in a rotating shallow-water layer. Dyn Atmos Ocean 49:1–24

Tomczak M (1988) Island wakes in deep and shallow-water. J Geophys Res-Oceans 93:5153–5154

White L, Wolanski E (2008) Flow separation and vertical motions in a tidal flow interacting with a shallow-water island. Estuar Coast Shelf Sci 77(3):457–466

Wolanski E, Imberger J, Heron M (1984) Island wakes in shallow coastal waters. J Geophys Res-Oceans 89:553–569

Wolanski E, Asaeda T, Tanaka A, Deleersnijder E (1996) Three-dimensional island wakes in the field, laboratory experiments and numerical models. Cont Shelf Res 16:1437–1452

Zhang J, Childress S, Libchaber A, Shelley M (2000) Flexible filaments in a flowing soap film as a model for one-dimensional flags in a two-dimensional wind. Nature 408:835–839